

30832

NATIONAL LIBRARY
OTTAWA



BIBLIOTHÈQUE NATIONALE
OTTAWA

NAME OF AUTHOR *Richard Robert Smith*
TITLE OF THESIS *The Effect of Environment
on the Early Stages of
Metal Fatigue*
UNIVERSITY *of Alberta*
DEGREE FOR WHICH THESIS WAS PRESENTED *MSC in Engineering*
YEAR THIS DEGREE GRANTED *1976*

Permission is hereby granted to THE NATIONAL LIBRARY
OF CANADA to microfilm this thesis and to lend or sell copies
of the film.

The author reserves other publication rights, and
neither the thesis nor extensive extracts from it may be
printed or otherwise reproduced without the author's
written permission.

(Signed) *R. Smith*

PERMANENT ADDRESS:

*8608-157 Street
Edmonton
Alberta*

DATED *June 23* 1976

INFORMATION TO USERS

THIS DISSERTATION HAS BEEN
MICROFILMED EXACTLY AS RECEIVED

This copy was produced from a microfiche copy of the original document. The quality of the copy is heavily dependent upon the quality of the original thesis submitted for microfilming. Every effort has been made to ensure the highest quality of reproduction possible.

PLEASE NOTE: Some pages may have indistinct print. Filmed as received.

Canadian Theses Division
Cataloguing Branch
National Library of Canada
Ottawa, Canada K1A 0N4

AVIS AUX USAGERS

LA THESE A ETE MICROFILMEE
TELLE QUE NOUS L'AVONS RECUE

Cette copie a été faite à partir d'une microfiche du document original. La qualité de la copie dépend grandement de la qualité de la thèse soumise pour le microfilmage. Nous avons tout fait pour assurer une qualité supérieure de reproduction.

NOTA BENE: La qualité d'impression de certaines pages peut laisser à désirer. Microfilmée telle que nous l'avons reçue.

Division des thèses canadiennes
Direction du catalogage
Bibliothèque nationale du Canada
Ottawa, Canada K1A 0N4

THE UNIVERSITY OF ALBERTA

THE EFFECTS OF ENVIRONMENT
ON THE EARLY STAGES OF METAL FATIGUE

by

RICHARD R. SMITH



A THESIS

SUBMITTED TO THE FACULTY OF GRADUATE STUDIES AND RESEARCH
IN PARTIAL FULFILMENT OF THE REQUIREMENTS FOR THE DEGREE

of

MASTER OF SCIENCE
IN METALLURGICAL ENGINEERING

DEPARTMENT OF MINERAL ENGINEERING.

EDMONTON, ALBERTA

FALL, 1976

THE UNIVERSITY OF ALBERTA
FACULTY OF GRADUATE STUDIES AND RESEARCH

The undersigned certify that they have read, and
recommend to the Faculty of Graduate Studies and Research,
for acceptance, a thesis entitledThe Effects of.....
Environment on the Early Stages of Metal Fatigue.....
.....
submitted byRichard R. Smith.....
in partial fulfilment of the requirements for the degree of
Master ofScience.....

Michael L. Wayman
Supervisor
Gary Faulkner
F. Vittoria

Date *June 23/76*...

ABSTRACT

A high strength low alloy steel was fatigued in different environments and the surface examined in the scanning electron microscope to observe the development of surface damage in the early stages of fatigue. The wet hydrogen environment tended to produce a significantly coarser structure than the dry hydrogen environment. Extrusions were characteristic of this coarse type surface damage, whereas cumulus formations, which are likely to be regions of fine slip steps, developed extensively in the dry hydrogen.

It was found that the surface damage that occurs early in the fatigue life is very sensitive to minor variations in test conditions, and the possibility arises that trace amounts of oxygen play a major role in these minor variations.

ACKNOWLEDGEMENTS

The author is indebted to his supervisor Dr. M.L. Wayman for his assistance throughout the project.

My thanks to Dr. F.H. Vitovec for his advice and comments on the project, and for supplying the sample material and specifications.

Financial support from the Steel Company of Canada Limited is gratefully acknowledged.

TABLE OF CONTENTS

	<u>Page</u>
I. <u>INTRODUCTION</u>	1
II. <u>LITERATURE SURVEY</u>	3
III. <u>EXPERIMENTAL PROCEDURE</u>	9
MATERIAL	9
SPECIMEN PREPARATION	10
TESTING SYSTEM	12
TESTING PROCEDURE	14
EXAMINATION METHODS	15
IV. <u>RESULTS</u>	17
INITIAL MICROSTRUCTURE	17
SURFACE DAMAGE CAUSED BY FATIGUE	22
Types of Damage	22
Relation of Surface Damage to Microstructure	28
Effect of Environment on type of Surface Damage	28
Effect of Environment on Amount of Surface Damage	32
Effect of Surface Roughness	35
Tests Run to Failure	35
V. <u>DISCUSSION</u>	38
THE SCANNING ELECTRON MICROSCOPE	38
THE OXIDE LAYER	42
FATIGUE DAMAGE	43
EFFECT OF ATMOSPHERE COMPONENTS	46

TABLE OF CONTENTS (cont'd)

		<u>Page</u>
VI.	<u>CONCLUSIONS</u>	511\
VII.	<u>SUGGESTIONS FOR FUTURE WORK</u>	52
VIII.	<u>REFERENCES</u>	53
IX.	<u>APPENDIX I.</u>	56

LIST OF FIGURES

Figure		Page
1.	The test specimen after notching.	10
2.	The fatigue test system, showing the MTS, microscope, humidity gage and other components of the gas train.	13
3.	Showing the banded structure of the same X-70 material. Approximately 100X.	17
4.	Showing diamond pyramid hardness indents in the three phases present. 600X.	18
5.	Showing the etched pearlite at a magnification of 5,000 times.	19
6.	Showing the etched "martensite" at a magnification of 5,000 times.	20
7.	Extrusion formations at 700X fatigued in wet hydrogen. 4,000 cycles.	22
8.	Intermediate type of fatigue damage 700X wet hydrogen 4,000 cycles (top) dry hydrogen 4,000 cycles (bottom).	23
9.	Cumulus formations at 700X dry hydrogen 4,000 cycles.	24
10.	A well developed extrusion and the accompanying cracks or fissures. 5,000X 68,000 cycles fatigued in air.	25
11.	A cumulus formation at 5,000X. dry hydrogen 4,000 cycles.	26
12.	Intermediate fatigue damage. 5,000X dry hydrogen at 4,000 cycles.	27

LIST OF FIGURES (cont'd)

Figure		Page
13.	Cumulus formations in dry hydrogen. 4,000 cycles 400X.	30
14.	Extrusion formations in wet hydrogen. 4,000 cycles 400X.	31
15.	Slight fatigue damage. 400X wet hydrogen 4,000 cycles.	33
16.	Showing the path of a fatigue crack. fatigued in air 68,000 cycles 400X.	36
17.	Showing the path of a fatigue crack fatigued in air 68,000 cycles 3,000X.	37

INTRODUCTION

Metal fatigue is the disconcerting phenomenon that occurs when a metal product fails in service conditions in which the ultimate strength, and often, the overall yield strength of the metal has not been exceeded. It is the unconsidered factor when some old sailor says, "of course the rigging is sound, it's proved itself, why I've sailed her hundreds of hours in the heaviest of seas without a hint of trouble."

Metallurgists generally break this process down into three stages: initiation, the metal deformation prior to the formation of a crack; Stage I, the propagation of a crack on planes of maximum shear stress (slip planes); Stage II, the propagation of a crack on planes of maximum tensile stress.

Over the last thirty years almost all experimental studies have been done on Stage I and II crack propagation, and perhaps rightly so, as much of the fatigue life is spent in these two areas and information such as number of cycles to failure have a direct practical application. In research, studying this area has another advantage in that a crack has formed, i.e. a tangible defect with measurable characteristics, as distinct from the unfatigued metal.

However the generation of S-N curves is not going to lead to any complete explanation of the metal fatigue process. It is for this reason that it is necessary to probe the initiation stage, to perhaps delay the onset of the Stage I propagation.

Fatigue crack initiation in smooth, polished specimens involves the generation of a characteristically roughened surface topography, called herein, surface fatigue damage. This damage can eventually, by creating stress concentrations, develop into fatigue cracks. In the few articles that have been published on fatigue crack initiation there is general disagreement as to the effect that the environment has on the initiation. There is definitely an effect of environment on the total number of cycles to failure, but whether this affects only the Stage I and II propagation and not the initiation is not clearly defined.

Fatigue cracks usually initiate from the surface of the metal, as a result of localized reversed plastic deformation. The reactions at the gas-metal interface under the dynamic situation of plastically deforming metal, are likely to have an influence on the fatigue process. The prime object of this study, then, is to determine the effects, if any, due to changes in environment on the surface damage caused by fatigue in a high strength, low alloy, fine grained steel.

LITERATURE SURVEY

FATIGUE CRACK INITIATION IN GASEOUS ENVIRONMENTS

Starting with a clean smooth metal surface, the time between the first fatigue cycle and the formation of a propagating fatigue crack is termed the initiation (or nucleation) stage of the fatigue process.

In polycrystalline copper at low stress (fatigue life 10^6 - 10^7 cycles) specimens showed slip markings in the first few cycles. These markings gradually became more numerous and intense with time. The most intense slip markings persisted through electropolishing which erased other slip lines, and thus were called persistent slip bands⁽¹⁾. At some undefineable point during the stress cycling these persistent slip bands can be termed cracks which spread to other grains of the material.

Other workers⁽²⁾ have found that extrusions, thin ribbons of metal protruding from the surface, form early in the fatigue life from regions where slip has occurred. Extrusions are formed in almost all materials over a wide range of temperature, and are often accompanied by intrusions, crystallographically oriented crevices or fissures, often parallel to the extrusions⁽³⁾.

In some materials, such as copper and brass, pores can be found in areas corresponding to persistent slip bands⁽⁴⁾. It is speculated that these pores are generated

in the persistent slip bands and link up to eventually form a crack⁽⁵⁾.

If the strain range of a metal (eg., copper) is increased during fatigue, with other factors held constant, the material hardens until a saturation stress is reached. Conversely, if the strain range is lowered, the metal will soften until a lower saturation stress is reached⁽⁶⁾. This phenomenon is reflected in the dislocation substructure that forms. It has been shown by Pratt⁽⁷⁾ that the dislocation cell size varies inversely with the saturation stress.

The dislocation substructure in the persistent slip bands appears to be characteristic of a higher strain amplitude than is the matrix between the slip bands⁽⁵⁾.

So the paradox arises as to why plastic deformation continues in the slip bands.

For high stacking fault (easy cross-slip) or wavy slip materials such as aluminum and copper, the dislocation structure of the persistent slip band appears "ladder like"⁽⁸⁾ looking in from the fatigued surface, and "cellular like" looking normal to the plane of the persistent slip band. For planar slip materials, (low stacking fault energy) the bulk dislocation array is planar and no persistent slip band structure in the usual sense is observed⁽⁹⁾.

Generally speaking, for face centered cubic metals having high stacking fault energy, the bulk dislocation substructure consists of prismatic dislocation loops at low stress amplitudes and cellular structure at high stress amplitudes. For planar slip materials multipole dislocation debris occurs at long life and planar arrays at short fatigue lives⁽¹⁰⁾.

At higher stresses (10^4 - 10^5 cycles to failure) Laird and Smith⁽¹¹⁾ found that for relatively pure aluminum, nickel, and copper, the fatigue crack formed in and propagated across grains except at the shorter life of this range, where the dominant crack always appeared to grow from a grain boundary. The tendency for intergranular fatigue cracks increases with increasing temperature and stress amplitude.

There is little doubt that the environment affects the fatigue life of metals. Sopwith and Gough⁽¹²⁾, in 1935, tested specimens in air and partial vacuum and found that it was necessary to have air present to obtain a short fatigue life. However, the effect of gaseous environments on fatigue crack initiation is far from resolved. There are those who say the environment has a major effect on initiation, and those who say it has no effect. Part of this discrepancy stems from the nebulous point, "at what length does a fatigue crack become a fatigue crack?", that is, whether the metal

is in the propagation stage of fatigue, or still considered to be in the initiation stage. Most of the debate arises from a lack of information, which in turn arises from the difficulty in gathering consistent data.

Thompson et al.⁽¹⁾ cycled copper in nitrogen and air and found, naturally, longer lives in nitrogen. By stopping the tests at different intervals and taking pictures it was concluded, although not with a great amount of confidence, that the absence of oxygen had little effect on the first appearance of the persistent slip bands, but the absence of oxygen did slow down the transition from persistent slip bands to cracks.

Broom and Nicholson⁽¹³⁾ working on aluminum found that changes in the environment affected initiation more than Stage I growth. Bradshaw and Wheeler⁽¹⁴⁾ found the opposite to be true.

The oxide layer has been object of much discussion with regard to initiation. It was found that fatigue life of aluminum increased with a decrease in atmospheric pressure⁽¹⁵⁾. The explanation for this was that in air the metal surface is strengthened by the oxide layer. This lowers the rate at which dislocations can escape, thus concentrating dislocations in the surface layer, enhancing the formation of voids and cavity dislocations. At low pressures the surface oxide formation is small allowing dislocations to escape, reducing the formation of voids and cavities; in addition the linkage of voids

is retarded. It was later found by Grosskreutz⁽¹⁶⁾, however, that the strength of the oxide layer increases in vacuum. This phenomenon is most probably caused by a decrease in the water content of the aluminum oxide. This appears to be a more likely explanation of the earlier results.

There are other less direct methods of determining the effect of environment on initiation. Hordon⁽¹⁷⁾ has concluded that because the crack nucleation phase was insensitive to variations in pressure and frequency, the initiation of fatigue cracks is not dependent on the surrounding gas environment.

Wadsworth⁽¹⁸⁾ and Frost⁽¹⁹⁾ found the fatigue limit for steel to be higher in a less aggressive environment. Cracks were found in the unfailed samples fatigued in the neutral environment at the fatigue limit. At this same stress in air, samples failed. Therefore they concluded that the stress to initiate a crack is not affected by the environment.

Wadsworth⁽²⁰⁾ viewed copper after 1.8×10^4 cycles at a stress where the life would be 5×10^5 cycles in air and 10^7 cycles in vacuum, and found that the samples appeared the same, except that the cracks in the samples fatigued in vacuum were slightly shallower.

Smith and Shahinian⁽²¹⁾ state that on nickel at

300° C severe rumpling was noticed in vacuum and not in oxygen at high pressures (10 torr), and that the formation of surface extrusions and intrusions was accelerated by oxygen.

The debate continues with different workers defining a crack at different stages. However, virtually all of the literature encountered reports the effects of the gaseous environment on crack initiation as a by-product of other investigations. That is, instead of the resolution of this problem being a center of concentration, dispersed bits of information are being generated while looking primarily at other phenomena. In this present project this problem was approached directly.

EXPERIMENTAL PROCEDURE

MATERIAL

The test material used was a low alloy, fine grained linepipe steel conforming to API standard 5LX-X70.

A tensile test showed a yield strength of 71,000 psi. and an ultimate strength of 89,000 psi. in the longitudinal direction, (parallel to the rolling direction).

The chemical composition of the steel in weight percent, as provided by the manufacturer, is:

	<u>Ladle</u>	<u>Check</u>
Carbon	0.10	0.09
Silicon	0.25	0.25
Manganese	1.48	1.48
Phosphorus	0.014	0.012
Sulphur	0.002	0.002
Niobium	0.05	0.04
Vanadium	0.10	0.10
Aluminum	0.033	0.035
Copper	0.31	0.33
Nickel	0.32	0.31
Carbon Equivalent		0.40

Check analysis performed by Chicago Spectro Ltd,
courtesy of Dr. F. H. Vitovec:

Carbon	0.09	0.09	Nitrogen	0.007	0.005
--------	------	------	----------	-------	-------

SPECIMEN PREPARATION

Samples of the steel were cut parallel to the rolling direction of the material. The specimens were an hourglass shape threaded at both ends, as described in Figure 1. Early specimens were not notched.

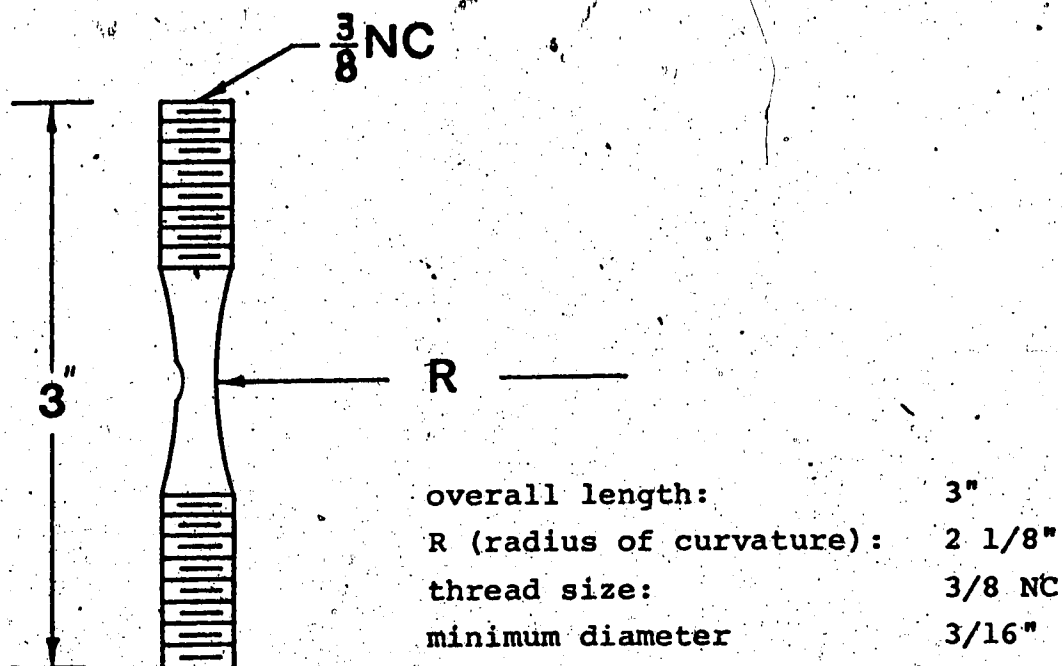


Figure 1. The test specimen after notching.

After machining, the gage lengths of specimens were ground in the lathe chucks with progressively finer silicone carbide paper (240-320-400-600) until a smooth finish was obtained.

The ends of the specimen were then ground to 600 grit and one end was further polished on the lapwheel to a six micron diamond finish. The polished end of the specimen was then etched in a 2% nital solution and placed in an

optical microscope to determine the banding orientation (see below). The other end of each specimen was marked with a vibrating engraver so the banding direction would be visible to the naked eye. A number was also engraved on the specimen for identification purposes.

Each specimen was placed in a Servo Met spark cutting machine and a notch was cut at the center of the gage length to a depth of approximately 0.03 inches using a 1/4" diameter brass rod as the cutting tool. The specimen was oriented so that the banding plane was normal to the base of the notch. Minimum power setting (range 7) was used to avoid creating cracks on the notch surface; no cracks were ever observed during later examination of the unfatigued specimens.

The specimens were then electropolished using a solution of: 133 cc. acetic acid, 20 cc. water, 25 grams chromic acid. The bath temperature ranged from about 12 to 30°C at a potential of 17 volts. The anode was an aluminum wire bent into an L shape with the short end of the L running parallel to the notch. The solution was cool at the start and slowly warmed up through the electropolishing. The specimen was considered polished when the notch displayed a mirror like finish. This usually occurred between 15-45 minutes, depending on the age of the bath and other variables. The specimens

were dimensionally analyzed using a Scherr Tumico Optical Comparator at a magnification of 20 times.

The presence of the notch causes a slight bending moment during axial loading and, all stresses reported here are nominal i.e. are based on the notched cross-section with no allowance made for the bending moment and stress concentration caused by the notch or specimen configuration.

TESTING SYSTEM

The fatigue tests were carried out on a model 810 material test system (MTS Systems Corp.) machine. This is a closed loop servo valve controlled hydraulic system. The system is very flexible, as different test parameters, such as frequency, amplitude, load or strain control are easily changed by means of the electronic control panel. A frequency of 1 Hz. was used for all tests.

An environment chamber was constructed of lucite and sealed over the MTS grips by two O-rings. Part way through the experimental procedure a gas sampling port was installed using a mylar seal.

For dry hydrogen testing, bottled (99.99%) hydrogen gas was passed through a cold finger liquid nitrogen trap (for condensing water) into a large pressure flask where a small relative humidity gage was installed. The gas was then routed through the sample chamber. The waste gas was bubbled through two oil traps to prevent any atmospheric gas from back-diffusing into the system.

All connections were made with standard tygon tubing.

For wet hydrogen testing the cold trap was filled with water and a heater installed externally to increase the relative humidity.

The gas sampling was done using a sealable valve type hypodermic syringe. The gas was then analyzed by using a Hewlett Packard Model 5830 A gas chromatograph.



Figure 2. The fatigue test system, showing the MTS, microscope, humidity gage and other components of the gas train.

TESTING PROCEDURE

Initially, push-pull fatigue tests were conducted to determine the fatigue life at various stress amplitudes. For these tests the spark machining of the notch had not been incorporated into the testing procedure and surface markings were not apparent prior to failure. This was attributed to the work hardened surface layer of the metal. It was thought that this layer, caused by the machining and grinding, was too thick to be removed by the light electropolish.

Spark cutting a notch and electropolishing the notch surface permitted the observation of fatigue damage after 2,000 cycles between a peak tensile stress of 73,000 psi. and a peak compressive stress of 31,000 psi. Test specimens were then run to failure under different environments. Some of these test samples were removed from the MTS, examined and photographed at various stages of the fatigue life. Large photographic collages of the notch surface were made. This allowed one to find the same area and be able to positively identify it a few thousand cycles later. Six samples were run to failure, three in air, one in dry hydrogen and one in oil. These initial tests showed a fatigue life of approximately 1×10^4 cycles at +73,000 to -31,000 psi.

Since one of the prime objectives of this study was to determine the effect of environment on the develop-

ment of surface fatigue damage, limited cycle tests were conducted. From the initial tests it was determined that 4,000 cycles between 73,000 psi. tension and 31,000 psi. compression gave a large number of fatigue markings and no multigrain fatigue cracks. Thus twenty-five specimens were prepared for these limited cycle tests, which were performed in three atmospheres: wet and dry hydrogen, and air.

The environment was monitored by the relative humidity gage. After purging the system with the prepurified hydrogen to a point where the humidity approached zero or 100% the test was considered ready to run. Gas analysis was introduced at specimen number 20 in order to certify whether or not this control was sufficient. A list of tests run is given in Appendix I.

EXAMINATION METHODS

Optical microscopy was used to compare the results of the scanning electron microscope and microstructural examination of the original material. A special optical microscope stage was built on the MTS in order to monitor the fatigue damage as the tests progressed.

A special stage was also built on the ISI Mini Sem-5 scanning electron microscope in order to accommodate whole fatigue specimens. Thus a sample could be fatigued, examined, and the fatigue then continued. This turned out

to be a much superior method than the mounting of the optical microscope for the viewing of progressive damage.

A standardized procedure was adopted for viewing specimens in the SEM. This consisted of placing the middle of the notch in the center of the field of view at a magnification of 30X, then using higher magnifications to examine this area in more detail. Furthermore large collages of photographs were taken so as to cover approximately 25-50% of the width of the notch at the approximate region of minimum cross-section. This ensured that observations on all specimens were unbiased, representative and corresponded to the same stress amplitude.

Use of the transmission electron microscope was also attempted. Unfortunately the small waist of the hourglass sample made replication very difficult, and the higher magnification supplied by the transmission electron microscope was not needed for this study. Thus, the primary tool for examining the metal specimens was the scanning electron microscope.

RESULTS

INITIAL MICROSTRUCTURE

Samples of the as received X-70 steel were prepared and examined to ascertain the microstructure. A square metallographic sample was prepared, carefully polished on three sides and then etched in a 2% nital solution. This sample showed that the steel had a banded structure similar to Figure 3.

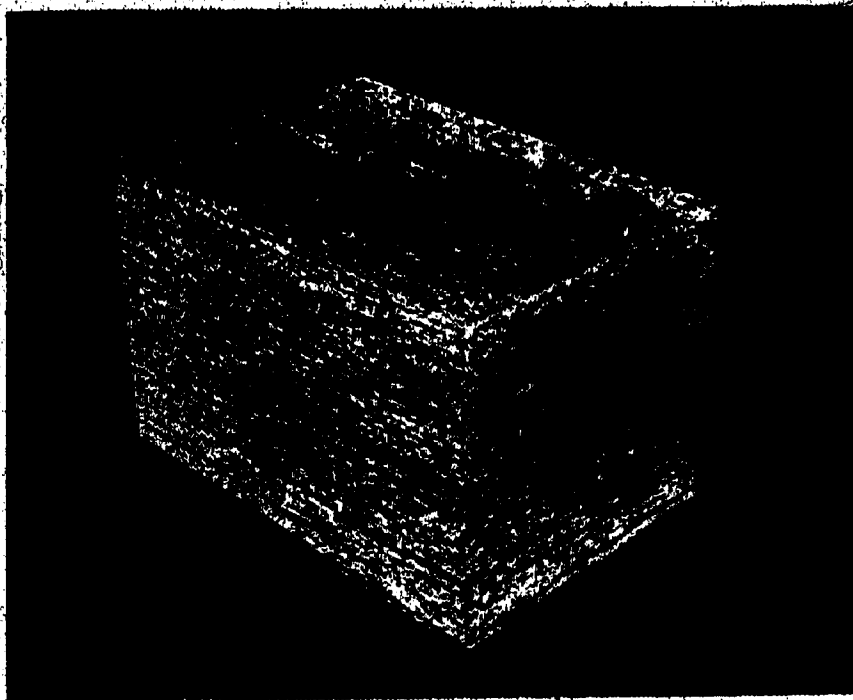


Figure 3. Showing the banded structure of the same X-70 material. Approximately 100X.
Courtesy of Dr. F. H. Vitovec.

The bands were spaced approximately 25-75 microns apart oriented parallel to the rolling plane and rolling direction of the original material.

The matrix material was ferrite with the bands made up of either pearlite or a "martensite" type structure. Using the nital etch and a light optical microscope the pearlite appeared darker than the ferrite matrix while the "martensite" appeared more dispersed and had a much finer grain size (Figure 4).



Figure 4 Showing diamond pyramid hardness indents in the three phases present. 600X.

At a power of 5,000 times the image in the scanning electron microscope clearly shows pearlite with the customary lamellar structure (Figure 5). The ferrite and the "martensite" appear similar, except that the ferrite is attacked more rapidly by the etch giving the "martensite" a slightly elevated surface (Figure 6).



Figure 5. Showing the etched pearlite at a magnification of 5,000 times.

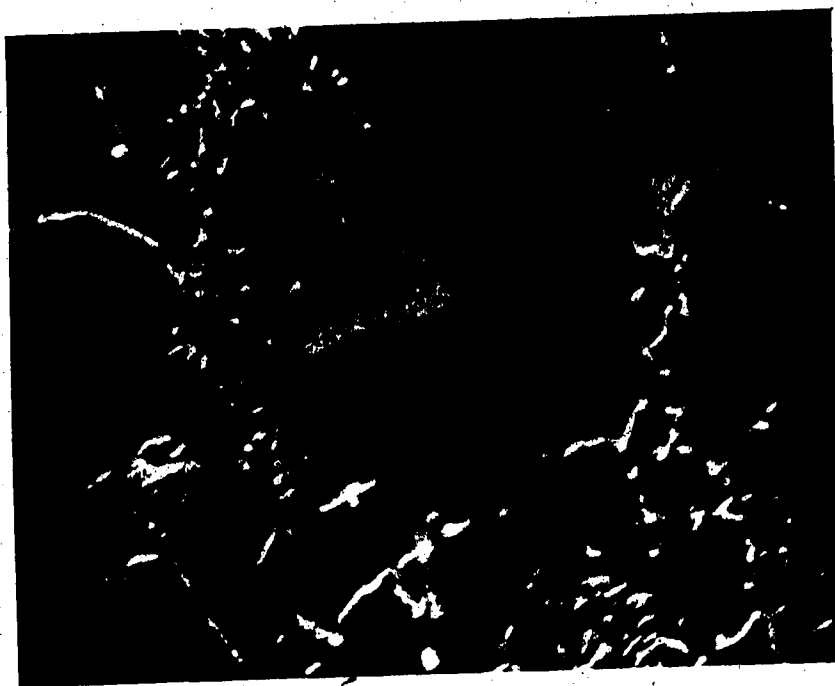


Figure 6. Showing the etched "martensite" at a magnification of 5,000 times.

Diamond Pyramid Hardness tests of the phases were performed with a Reichert Microhardness tester. The average DPH values in kg/mm^2 are as follows:

Indentation load	Ferrite	Pearlite	"martensite"
20 grams	192	283	386
35 grams	205	248	336

The hardness values for ferrite and pearlite correspond well with reported data⁽²²⁾. The unresolved phase has been termed "martensite" as its hardness agrees with the hardness for martensite as given by Bain⁽²³⁾. However, only electron transmission microscopy would provide positive identification of the phase.

SURFACE DAMAGE CAUSED BY FATIGUE

Types of Damage:

Scanning electron microscopy of the surface of the fatigued samples revealed that the surface damage caused by fatigue developed as a spectrum with one type of damage merging into another. At one extreme of this spectrum was extrusion formations and, at the other, wispy cloud-like structures which shall be referred to as cumulus formations. The majority of the fatigue markings were intermediate, possessing some characteristics of both the extrusion and cumulus formations. Figures 7 to 9 show the spectrum of fatigue damage that was seen to occur while fatiguing in the different environments.



Figure 7. Extrusion formations at 700X
fatigued in wet hydrogen. 4,000 cycles.

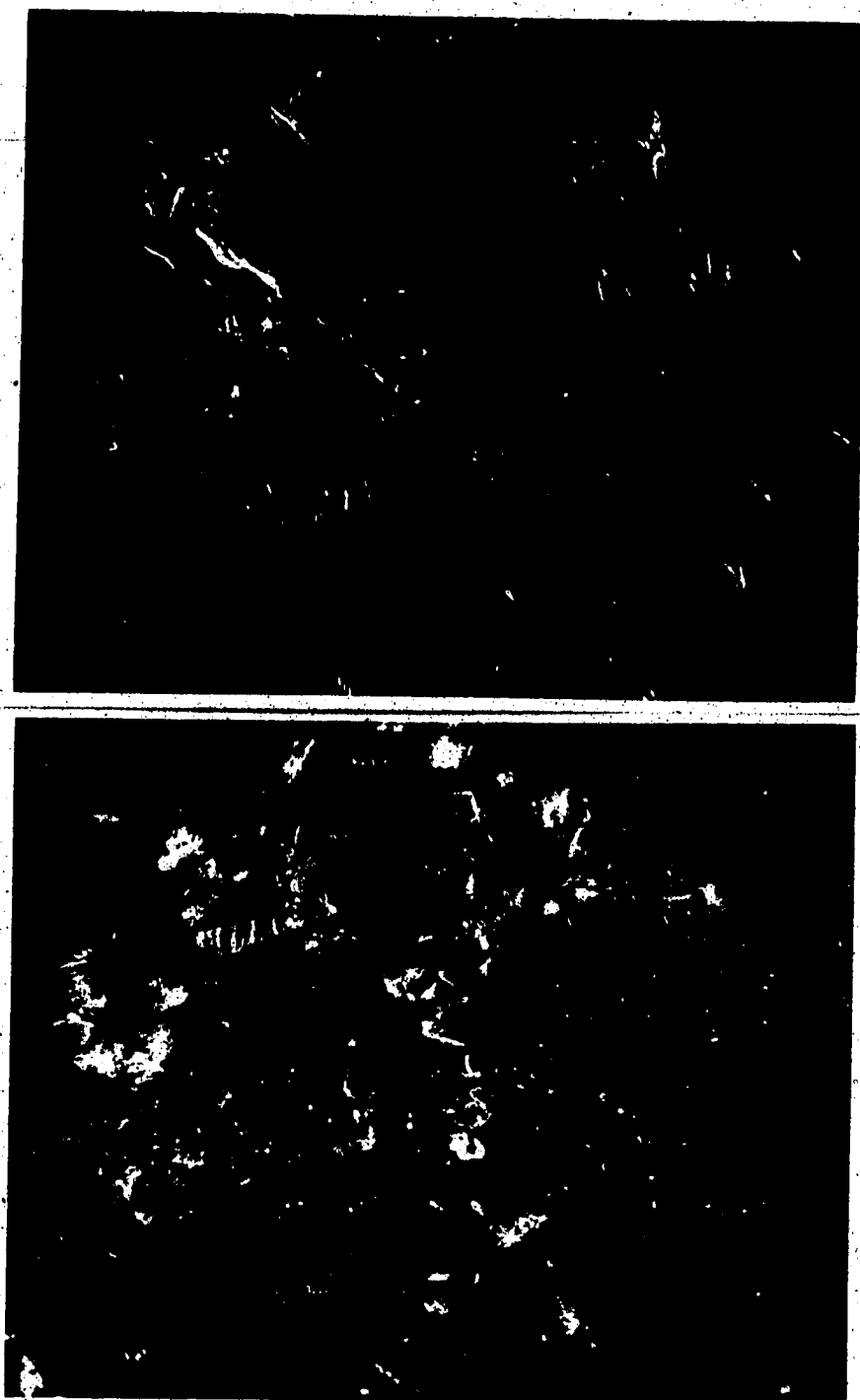


Figure 8. Intermediate type of fatigue damage 700X
wet hydrogen 4,000 cycles (top)
dry hydrogen 4,000 cycles (bottom).



Figure 9. Cumulus formations at 700X
dry hydrogen 4,000 cycles.

The main characteristics of these types of damage will first be described. This will be followed by descriptions of the fatigue test conditions which caused specific surface appearances.

Extrusions started early in the fatigue test as small bumps or ridges on the metal surface. As the test continued some of these became well defined

extrusions which kept growing in length and amount of metal extruded. This continued until a crack developed in or beside the extrusion. These cracks were usually in line with the extrusion, however Figure 10 shows many small cracks at slightly different angles than the extrusion. Cracks continued to grow and link together until, out of many possibilities, a fatal crack formed.

Extrusions generally formed in groups where they tended to be parallel to one another at an angle to the normal stress. However the intersection of extrusions at right angles was not uncommon. In these cases one extrusion would arrest the growth of the intersecting extrusion as shown in Figure 10.



Figure 10. A well developed extrusion and the accompanying cracks or fissures. 5,000X
68,000 cycles fatigued in air.

The cumulus formations appeared similar to small thin cumulus clouds as viewed directly overhead. They were globular in shape and were sharply distinct from the background. As the cycling proceeded the cumulus formations did not increase in size as the extrusion formations did, but did appear to grow somewhat less hazy as the test continued. New formations continued to appear as the number of cycles increased. When viewed at high magnification with the scanning electron microscope the cumulus formations exhibited a mixed criss-cross structure as seen in Figure 11.

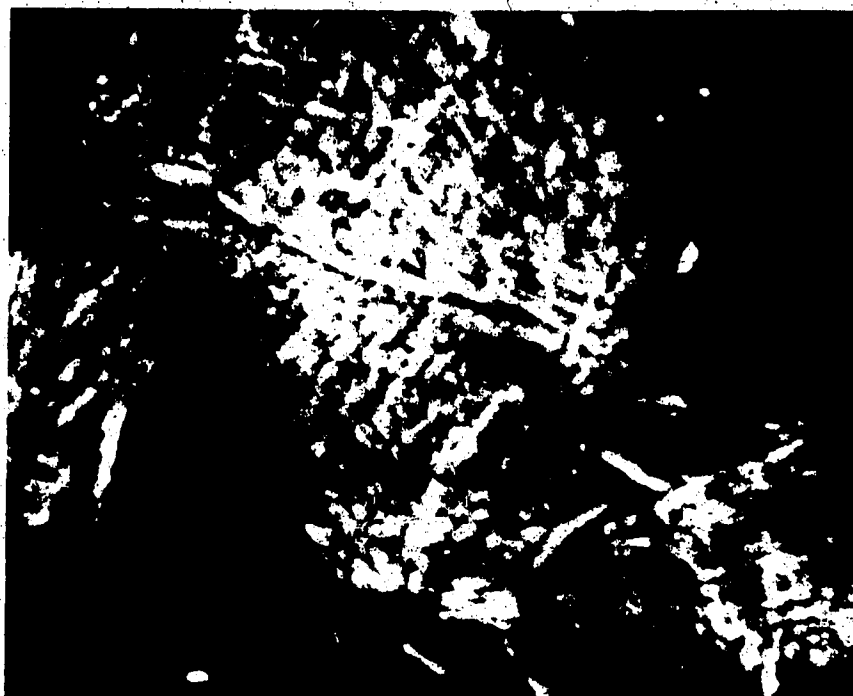


Figure 11. A cumulus formation at 5,000X.
dry hydrogen 4,000 cycles.

A large portion of the fatigue damage was intermediate in nature. Some areas showed an extrusion-like structure with a random orientation (the extrusions were often distorted when compared to the long, even extrusions of the extrusion formations); in other areas the damage had definite boundaries and orientation, sometimes resembling expanded mesh steel (Figure 12).

As will be discussed later all fatigue samples showed the entire range of features to varying extents.



Figure 12. Intermediate fatigue damage 5,000X.
dry hydrogen at 4,000 cycles.

Relation of Surface Damage to Microstructure:

As previously noted, large collages of the fatigued metal surface were produced. These pictures showed fatigue damage but no significant microstructure since the specimen surfaces had been electropolished prior to fatigue. However, one of the fatigued specimens was etched and rephotographed. This clearly showed the pearlite and ferrite microstructure but erased most of the fatigue damage. Thus a transparency was placed over the "as fatigued" collage and some of the extrusion and cumulus formations were traced on the transparency. This was then superimposed over the etched collage allowing one to note the location of the fatigue damage in relation to the ferrite and pearlite.

Most of the extrusion-type formations occurred in the ferrite although there were a few instances of extrusions forming in the pearlite. All the cumulus type damage was seen to have originated in the ferrite.

Effect of Environment on Type of Surface Damage:

The 4,000 cycle tests, which were designed to distinguish the effect of environment of fatigue crack initiation, showed that in the samples fatigued in dry hydrogen cumulus formations predominated (Figure 13). The wet hydrogen environment produced mainly extrusion formations (Figure 14). The air environment seemed

to be less specific producing a balanced mixture of extrusions and cumulus formations. It must be noted that all types of damage were observed to some extent in all specimens and the above observations, while definite, are trends.



Figure 13. Cumulus formations in dry hydrogen.
4,000 cycles 400X.

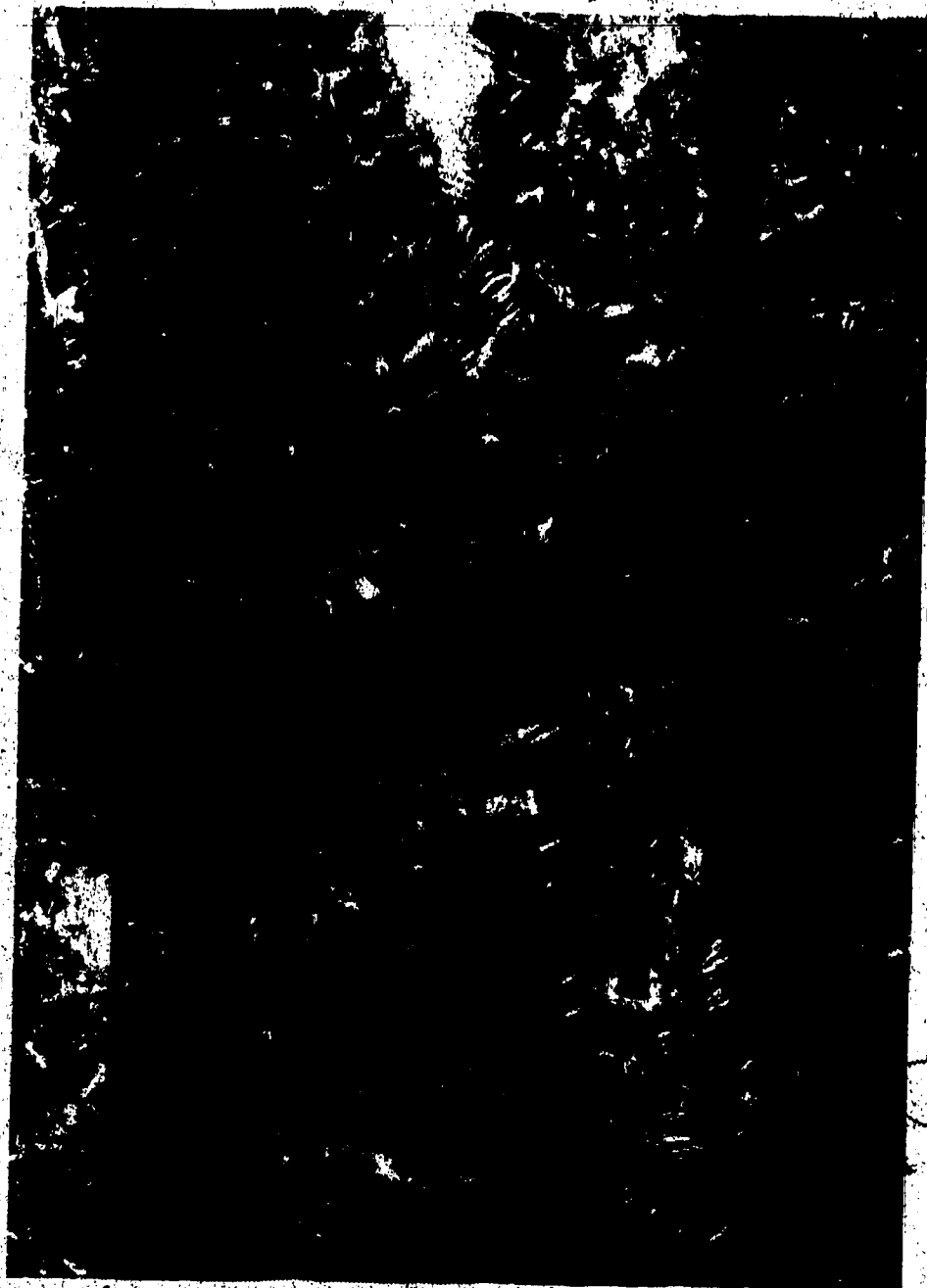


Figure 14. Extrusion formations in wet hydrogen.
4,000 cycles 400X.

Effect of Environment on Amount of Surface Damage:

The amount of fatigue damage was considerably less consistent than the type of damage. The early tests showed that an atmosphere of dry hydrogen would produce the most damage, air would produce the least amount of damage and wet hydrogen was somewhere between the two extremes.

It then became apparent that if two tests were run successively in dry hydrogen the second test showed almost no damage. If three tests were run successively in wet hydrogen the first showed a normal amount of fatigue damage, the second two showed virtually no damage (Figure 15). This seemed to indicate that on start-up tests some air was still present in the environment system. Tests were therefore conducted in which the system was purged hours before the stress cycling was started. Some of these tests showed a normal amount of damage and some showed almost none.

Gas chromatographic analysis of the environment indicated that the system stabilized approximately one hour after the gas flow started. In the stabilized condition the dry hydrogen atmosphere had a nitrogen content of less than 0.4% and the wet hydrogen atmosphere had a nitrogen content of less than 0.2%. In both cases

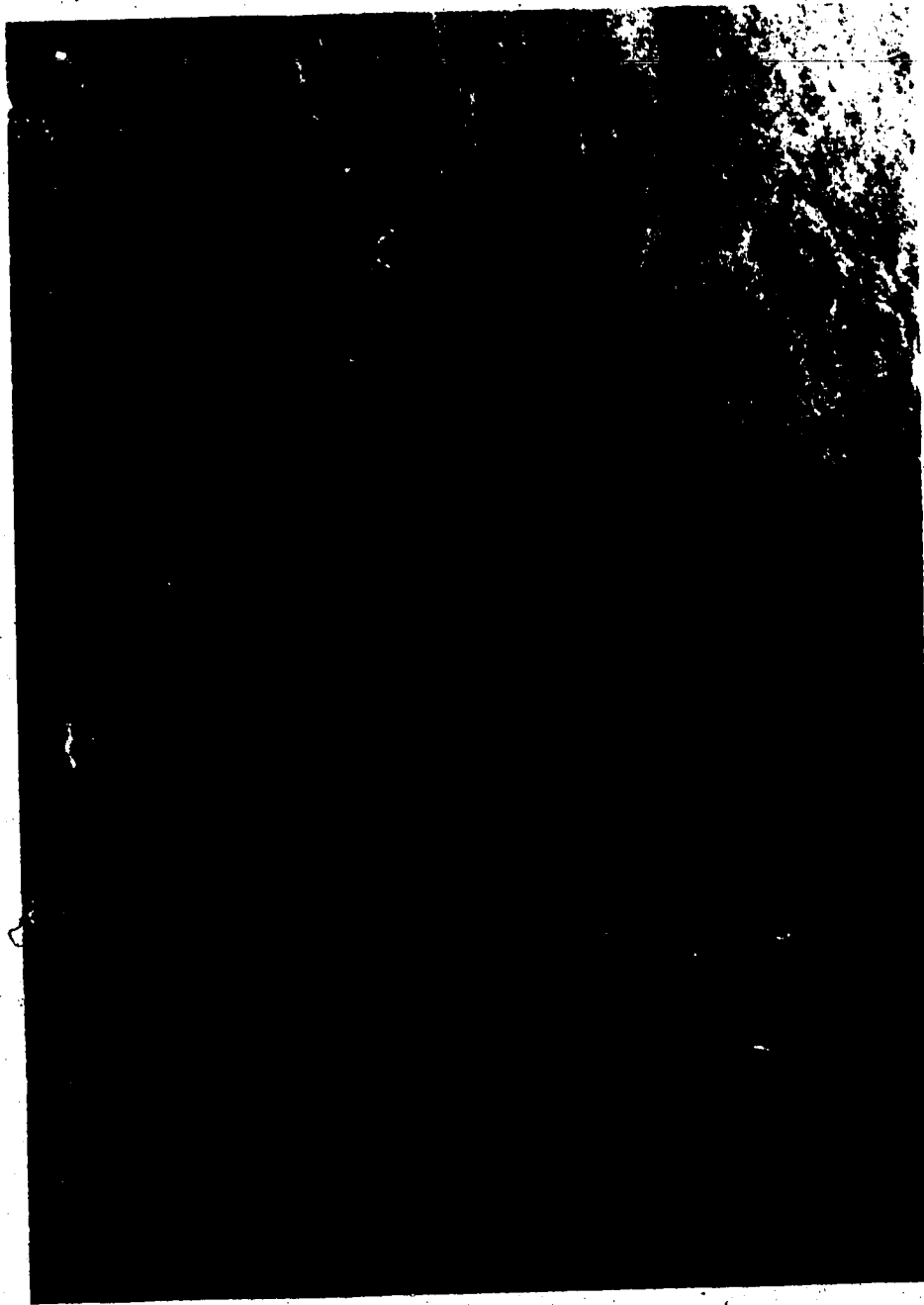


Figure 15. Slight fatigue damage. 400X
wet hydrogen 4,000 cycles.

the oxygen was below the detection limit of the gas chromatograph. Assuming that the nitrogen was from the atmosphere, it would follow that one fifth as much oxygen would also be present.

There are many variables in the material-test-environment which could have been responsible for this inconsistency.

Spark cutting left a variable surface finish which required different amounts of electropolishing to remove. The electropolishing itself varied somewhat in temperature, anode-cathode distance, and age of the bath. The time difference between electropolishing and use of the sample varied. This could have allowed a different type of oxide film on the surface.

The samples could have been bent somewhat in the machining process. This would then lead to asymmetry in gripping the sample, which could have left the notched side of the specimen under compressive or tensile residual stress. No visible bending was observed.

Since the MTS is a closed loop servo valve system some changes in the stress wave imposed on the sample could have resulted from a change in oil temperature, or the amount of dither.

It is assumed that most of the residual air diffused in through the tygon tubing. Changes in the amount of positive hydrogen pressure could have an effect on the amount of residual air.

The Effect of Surface Roughness:

Although all samples were electropolished to a mirror-like finish, some differences in the surface texture were apparent. This surface texture had a marked effect on the fatigue damage. Those samples having a pebble-like surface at a magnification of four hundred times showed shorter chunkier extrusions, and the cumulus formations were smaller and not as well formed. Surfaces which appeared smooth at the same magnification gave way to the type of fatigue damage previously mentioned.

Tests Run to Failure:

The results of tests that were run to failure agreed with expectations based on the type of fatigue damage visible at 4,000 cycles. On a sample tested in dry hydrogen, which failed at 24,000 cycles, the surface showed very few subsidiary cracks. The wet hydrogen sample failed at 19,500 cycles. This surface showed a significant number of subsidiary cracks. The sample fatigued in air failed at 11,500 cycles and, like the wet hydrogen sample, it showed many subsidiary cracks. Although there were not enough tests done to be conclusive these tests indicate as expected that the cumulus type formations are not as able to initiate a fatigue crack as are the extrusion type formations.



Figure 16. Showing the path of a fatigue crack.
fatigued in air 68,000 cycles 400X.

A sample that was run to failure was etched in a 2% nital solution and viewed in the scanning electron microscope (Figure 16). This showed that the propagating fatigue crack generally tended, as much as possible, to avoid crossing the pearlite. This was not a fixed rule, as Figure 17 shows a fatigue crack crossing the pearlite both across and between pearlite colonies. It is important to note here that the structure below the surface is unknown and could be different than that on the surface.



Figure 17. Showing the path of a fatigue crack fatigued in air 68,000 cycles/3,000X.

DISCUSSION

THE SCANNING ELECTRON MICROSCOPE

The scanning electron microscope (SEM) was used extensively for studying the metal surface. The large depth of field, high resolution, easy sample preparation and range of magnification made this tool superior to both the optical and the transmission electron microscopes for the purposes of this study. However, the image presented on the cathode ray tube of the SEM is an artificial representation of the metal surface and consequently some of the operational characteristics of the microscope affecting the results of this work must be considered before discussion of the results.

The basic operation of the scanning electron microscope (24,25) depends on the ability of local areas on the metal surface to emit secondary electrons as a result of a beam of primary electrons striking the surface in a raster pattern. An area of high secondary electron emission is represented on the cathode ray tube by a brighter spot than an area of low emission. Thus the image of the specimen is in fact a map of the intensity of secondary electron emission. Fortunately this is an excellent approximation of the surface, as a hole or groove does not allow electrons to be emitted as well as does a ridge or hill on the sample surface. Sharp thin protrusions or edges are the best emitters. This

gives well defined outlines to the topographic surface features.

In the SEM, the electron collector (usually less than 0.5 inches in diameter) is positioned to one side of the sample. When viewing a particular surface feature the side that faces the collector will appear brighter than the side that faces away from it. There is a bias voltage applied between the collector and the sample causing electrons to be drawn towards the collector. The emitted electrons have less chance of being reabsorbed by the metal surface if they can go directly to the collector rather than curving around some topographic feature, thus the image appears to have shadows as if light were shining on the surface from an angle.

When the beam of primary electrons impinges on the sample the electrons penetrate the surface. Some of these electrons are backscattered, some are emitted as secondary electrons and others flow from the specimen to ground as "sample current". The secondary electrons are of a low energy usually less than 50 eV. and are caused by inelastic collisions between the primary (and/or backscattered) electrons and the atoms in the specimen. The "escape depth", or "information depth" from which the secondary electrons are emitted is in the order of 100-500Å for most metals⁽²⁶⁾. An increase in the voltage of the primary electrons (i.e. the

accelerating voltage of the SEM) causes more secondary electrons to be generated and a deeper depth of penetration. However, the deeper into the metal the secondary electron is generated the less chance it has of being emitted from the surface. Thus as the beam voltage increases, the secondary electron emission increases to a maximum, beyond which it decreases.

Using this information, it is easily seen why the surface features oriented at other than right angles to the primary beam are stronger emitters than surfaces of normal incidence. The region in the sample where the primary beam excites secondary electrons is closer to a free surface allowing more secondary electrons to be emitted. This is the most important cause of topographic contrast in the SEM.

As the atomic number of the sample decreases, the penetration of the electron beam increases, thus fewer secondary electrons are emitted unless a lower accelerating voltage is used.

The other factor which affects the emission of secondary electrons is the ease with which they can leave the sample surface. Insulators, such as Al_2O_3 , have the highest yield of secondary electrons emitted per unit of primary electrons. The semiconductors have a somewhat lower yield and metals have the lowest.

However, insulators allow an electrical charge to build up on the specimen. If the secondary electron emission is less than the primary electron beam minus the back scattered electrons, the sample will become charged negatively repelling the incident primary beam. The sample will accumulate a negative charge until the energy of the incident electrons approaches zero. If the ratio of the secondary electron emission to primary electrons minus the backscattered electrons is greater than one the sample will charge positively. Clearly, the potential of the incident electrons will increase until the penetration becomes so great that an equilibrium is reached. This equilibrium primary electron beam voltage commonly lies in the range of 1 to 10 keV.

These, then, are the factors which must be considered in interpreting SEM images of the surfaces of fatigued specimens.

Before discussing the surface observations, it is necessary to consider the nature of electropolished steel surfaces and, in particular, the characteristics of the thin oxide layers which are likely to be present.

THE OXIDE LAYER

There are six different types of iron oxide that form on steel⁽²⁷⁾: two crystalline structures for FeO , one for Fe_3O_4 , and three for Fe_2O_3 . Since water was used in the electropolishing solution and also to rinse the samples immediately after the electropolishing, the list of possible reaction products can be extended to include all possible forms of hydroxides and hydrated iron oxides.

It is known that⁽²⁸⁾ after exposure to air, iron develops an oxide film of 6 to 12 Å in a few seconds and reaches a limiting thickness of 25 to 40 Å after several months. Only direct analysis would provide conclusive identification of the oxide film formed on the specimens pertaining to this work because of the many variables affecting the formation of the oxide. However, in the light of a vast amount of previous work^(29,30), it is reasonable to assume that the oxide film before fatiguing is made up of Fe_3O_4 under a layer of a spinel-type Fe_2O_3 containing some water. The relative thicknesses of the two layers cannot be estimated with any confidence. In addition oxide whiskers may form as discussed below.

It is now possible to interpret the SEM images of the fatigue damage.

FATIGUE DAMAGE

Extrusions were identified as such by taking sets of two pictures differing only in the incident angle of the electron beam. These stereo pairs clearly showed material jutting out of the fatigued surface when observed in the stereo viewer. Thus the interpretation of the extrusion appearance is straightforward.

More difficult to interpret, is the appearance of cumulus formations, the globular areas of enhanced emission on the metal surface. Within these overall bright areas were lines or troughs as seen in Figure 11. This could indicate that the metal surface had a large number of sharp topographical features, eg. finely spaced slip steps. This is certainly the most obvious interpretation of the cumulus formations, however it is not the only one.

Other possible explanations invoke the characteristics of the surface oxide layer. Firstly, the oxide could be much rougher in some areas than in others, giving bright regions in the SEM. Secondly, whiskers of metal oxide have been shown to occur on iron. Much wider and longer oxide whiskers form in a 10% water-Ar system than a dry (-79°C dew point) oxygen environment at 450°C ⁽³¹⁾. If whiskers started to grow on the oxide they would be

expected to be thinner and sharper in the dry hydrogen. This would cause brighter areas in the SEM, hence the appearance of cumulus formations.

Alternatively, different oxides could be nucleated in different areas. Since the amount of secondary emission changes with the properties of the oxide, this must be considered. The two oxides have very different electrical properties, Fe_3O_4 having an electrical conductivity of 10^4 mho/m while Fe_2O_3 is listed at 3.7×10^{-3} mho/m (27). Since secondary electron emission is higher for insulators than for metals, a thick film of Fe_2O_3 would appear brighter than Fe_3O_4 . However, it would seem that if the oxide layer was undergoing a reaction during fatiguing the presence of dry hydrogen would not enhance the formation of Fe_2O_3 , as some form of oxygen must be available to oxidize the iron. Therefore the cumulus formations (observed predominantly after fatigue in dry hydrogen) are not simply areas of thick Fe_2O_3 .

Another interesting possibility is that the cumulus formations have their characteristic appearance as a result of a combination of surface roughness due to slip steps and voids between the oxide film and the metal surface. Normally, the thin oxide layer does not build up a substantial charge because of the large oxide-metal interface area per volume of oxide. When an electrical charge starts to build up it need only traverse a

small distance in the oxide before reaching the conductive metal. Therefore, it is seen that a number of voids under the oxide will decrease the interface area and allow a larger charge to build up in the oxide. This could appear as an area of enhanced secondary electron emission.

It is believed that the most realistic explanation for the cumulus formations would be fine slip steps, most likely enhanced by voids at the oxide-metal interface.

The previous chapter showed that cumulus formations were enhanced by the dry hydrogen atmosphere while extrusions were more common on the metal surface that was fatigued in wet hydrogen. The reasons why the environment affects the surface damage will now be discussed.

EFFECT OF ATMOSPHERE COMPONENTS

If the oxide layer were thin enough, the absence of water would allow hydrogen to diffuse nearer to the metal since water is a very polar molecule and would probably form a physically adsorbed layer on the oxide surface. Thus, there would be more hydrogen-metal interaction, especially in areas of intense slip where freshly exposed metal and local high temperatures could possibly promote the formation of atomic hydrogen. The atomic hydrogen could embrittle the metal making the slip steps small and sharp, as there would be less plastic deformation involved in the slip process. As soon as a slip step appeared the hydrogen would not only chemisorb on the slip step but diffuse down the slip plane impeding dislocation motion. This would promote the formation of many small slip steps in the dry hydrogen environment in agreement with the appearance of cumulus formations. In wet hydrogen, these effects are likely to be masked by the effects of water.

The effect of water is to greatly enhance the development of extrusions. The effect appears to be the inhibition of the fine slip which is expected in the material due to its high dislocation density and high density of fine carbide particles⁽³²⁾. Extrusion

formations are categorized by severe "damage" in a few places, rather than slight damage in many places. This could happen by a corrosion reaction, by a surface reaction or alternatively, as a result of changes in the mechanical properties of the oxide.

The extrusions are most probably the result of irreversible slip caused by the freshly exposed metal reacting with the water vapour and/or residual oxygen. This would prevent the slip step from re-entering upon application of opposite loading in the fatigue cycle. Unlike the hydrogen penetration that was discussed earlier, this reaction would only occur on the surface of the slip step and thus would act only to prevent slip in one direction. This type of behavior would more likely occur in wet hydrogen than in dry hydrogen, therefore in wet hydrogen more extrusion formations would be expected, as is observed. Furthermore, this explains why more careful purging of residual oxygen from the system gave rise, albeit irreproducible, to less fatigue damage.

The possibility also exists that a corrosion mechanism may be responsible for, or may assist the formation of extrusions. It has been shown in several previous studies^(33,34) that at some point above 60% relative humidity, water can condense out in crevices and fissures which have small radii of curvature. This is because of the lowering of the equilibrium

saturation vapour pressure in the presence of a sharply curved surface. Such an effect could happen in the present case if the fatigue process caused features to form that had sharp radii of curvature, for example at intrusions, at extrusion-surface intersections or by a cracking of the oxide film. It has been observed that small fissures form at the edge of the persistent slip bands. Water could then condense in these fissures in sufficient volume to cause an electrolytic stress cell with the work hardened (slip band) side of the fissure being more anodic than the opposite side. This would initiate a fatigue crack and help to propagate it. Operation of this mechanism necessitates some oxygen dissolving in the condensed water, either from the surface, or, as discussed below, from the environment.

The presence of liquid water on the metal surface makes possible a Rebinder mechanism by which a liquid adsorbing on a solid (as in fissures) may lower the surface energy of the solid sufficiently to alter its mechanical properties. This could cause more small cracks to form on samples fatigued in wet hydrogen, whereas more surface plastic deformation would occur in dry hydrogen.

It has been shown that aluminum experiences a ten fold increase in fatigue life when fatigued in vacuum, as opposed to ambient air⁽¹⁷⁾. Later it was discovered that the Al_2O_3 layer on the aluminum surface increased

in strength and stiffness if placed in an environment of low water vapour pressure⁽¹⁶⁾, and that this, was responsible for the environmental effect on fatigue behavior on aluminum. This probably also applies to iron, as the Fe_3O_4 , and likely the Fe_2O_3 forming on iron at room temperature have spinel structures⁽³⁰⁾, as does the aluminum oxide⁽³⁵⁾.

A stiff strong layer of oxide, such as might form in dry hydrogen, would oppose the formation of slip steps, especially large slip steps as they would tend to stretch the oxide layer. However, the Pilling-Bedworth ratios for Fe_2O_3 and Fe_3O_4 are greater than 2⁽³⁶⁾, and it has been shown that oxide forms on iron under residual compressive stress approaching 40,000 psi.⁽³⁷⁾ Therefore many small slip steps would be expected in this case (especially in random orientation) as it would allow the oxide film to stretch out, although not enough to put it significantly into tension.

According to this model an environment of wet hydrogen would render an oxide film weak enough to rupture in various places allowing large slip steps and the customary extrusions to form.

The above model is further strengthened by reports of some surface observations on aluminum with a natural oxide layer (less than 50 Å). It has been shown⁽¹⁶⁾

that the slip lines observed after cycling in vacuum (an environment of low water vapour pressure) are more closely spaced than those found after cycling at atmospheric pressure (an environment of higher water vapour pressure).

Considering all of the different mechanisms a logical sequence would be as follows: the oxide film would first be weakened by the presence of water vapour in the environment of wet hydrogen. This would allow the oxide film to break upon the formation of slip steps. The slip would continue to operate on these persistent slip bands as there would be no mechanism present to impede their motion. The formation of extrusions could be enhanced by the reaction of the slip step and the residual oxygen or some complex reaction of the oxide film. An electrolytic cell could also be set up in the fissures that were often seen along side the extrusions, but the major factor for the formation of the extrusions would be the weakening of the oxide layer.

The dry hydrogen atmosphere would tend to strengthen the oxide film as the dew point in the sample chamber approached -196°C (as this was the temperature of the liquid nitrogen cold trap). Again the presence of the hydrogen could serve to impede the dislocation motion in the slip bands, but the major factor in the development of many fine steps instead of fewer coarser steps would be the strong rigid oxide layer.

CONCLUSIONS

1. When a high strength low alloy steel is fatigued in wet hydrogen, the surface damage consists largely of extrusions.
2. When the same steel is fatigued in dry hydrogen a cumulus-appearing feature predominates.
3. It is likely that the appearance of the cumulus formations in the SEM is due to patches of very fine slip perhaps associated with voids at the oxide-metal interface.
4. The effect of environment on surface fatigue damage can be largely explained if, as is the case for aluminum, water lowers the strength and stiffness of the surface oxide film.
5. There are indications that the presence of oxygen in the environment increases the amount of surface fatigue damage.
6. The surface fatigue damage that occurs during the initiation stages of a fatigue crack is very sensitive to minor variations in the test conditions.

SUGGESTIONS FOR FUTURE WORK

1. If a similar project should ensue, any modification that would lead to a more rigorous standardization of the test conditions would be beneficial. These could include:
 - i. liquid metal grips on the MTS to avoid the possibility of imposing individual bending moments on the test specimens.
 - ii. elimination of the tygon tubing to insure less contamination in the environment system.
 - iii. installation of an in-line gas analyser for meticulous monitoring of the gas environment.
2. The properties of the iron oxide appear to have a major effect on the fatigue damage. It would be advantageous to know how the properties change as a function of the environment.
3. A surface damage study on the fatigue crack initiation of gold would be interesting, as the metal surface does not have the added complication of an oxide layer.

REFERENCES

1. Thompson, N., Wadsworth, N., and Louat, N., Phil. Mag., 1, 113, (1956).
2. Forsyth, P.J.E., Nature, 171, 172, (1953).
3. Coffin, L.F.Jr., Ann. Rev. in Mat. Sci., 2, 312, (1972).
4. Wood, W.A., Cousland, S., and Sargant, K.R., Acta Met., 11, 643, (1963).
5. Grosskreutz, J.C., in Metal Fatigue Damage-Mechanism, Detection, Avoidance and Repair, ASTM STP 495, 1971, pp. 5-60.
6. Coffin, L.F.Jr., and Tavernelli, J.F., Trans. Met. Soc. AIME, 215, 794, (1959).
7. Pratt, J.E., J. Materials, 1, 77, (1966).
8. Lukas, P., and Klesnil, M., in Corrosion Fatigue: Chemistry, Mechanics and Microstructure, O.F. Devereux, A.J. McEvily, and R.W. Staehle, eds., NACE, 1972, pp. 118-132.
9. Lukas, P., and Klesnil, M., Phys. Stat. Sol., 37, 833, (1970).
10. Feltner, C.E., and Laird, C., Trans. Met. Soc. AIME, 242, 1253, (1968).
11. Laird, C., and Smith, G.C., Phil. Mag., 8, 1945, (1963).
12. Gough, H.J., and Sopwith, D.G., J. Inst. Met., 56, 55, (1935).
13. Broom, T., and Nicholson, A., J. Inst. Met., 89, 183, (1960-61).




14. Bradshaw, F.J., and Wheeler, C., *App. Mater. Res.*, 5, 112, (1966).
15. Shen, H., Podlaseck, S.E., and Kramer, I.R., *Acta Met.*, 14, 341, (1966).
16. Grosskreutz, J.C., *Surface Sci.*, 8, 173, (1967).
17. Hordon, M.J., *Acta Met.*, 14, 1173, (1966).
18. Wadsworth, N.J., *Phil. Mag.*, 6, 397, (1961).
19. Frost, N.E., *App. Mater. Res.*, 3, 131, (1964).
20. Wadsworth, N.J., in Internal Stresses and Fatigue in Metals, G.M. Rassweiler and W.L. Grube, eds., Elsevier, 1959, pp. 382-396.
21. Smith, H.H., and Shahinian, P., in Effects of Environment and Complex Load History on Fatigue Life, ASTM STP 462, 1970, pp. 217-233.
22. See e.g. Flinn, R.A. and Trojan, P.K., Engineering Materials and their Applications, Houghton Mifflin, 1975.
23. Bain, E.C., and Paxton, H.W., Alloying Elements in Steel, American Society for Metals, 1961, p. 37.
24. Oatley, C.W., The Scanning Electron Microscope, Cambridge University Press, 1972.
25. Wells, O.C., Scanning Electron Microscopy, McGraw-Hill, 1974.
26. Pickwick, K.M., and Smith, E., *Micron*, 3, 224, (1972).
27. Samsonov, G.V., ed., The Oxide Handbook, IFL/Plenum, 1973.
28. Evans, U.R., The Corrosion and Oxidation of Metal: First Supplementary Volume, Arnold, 1968, p. 27.

29. Sato, N., Dudo, K., and Noda, T., Corrosion Sci., 10, 785, (1970).
30. Bloom, M.C., and Goldenberg, L., Corrosion Sci., 5, 623, (1965).
31. Gulbransen, E.A. and Copan, T.P., Nature, 186, 960, (1960).
32. See e.g. McCutcheon, D.B., and Jamieson, R.M., Low Temperature Thermal-Mechanical Treatment of Low Carbon Steels, presented at CIM Conference of Metallurgists, Halifax, Nova Scotia, Aug. 27-30, (1972).
33. Johnson, H.H., and Willner, A.M., App. Mater. Res., 4, 34, (1965).
34. Johnson, H.H., and Paris, P.C., Engng. Fracture Mech., 1, 3, (1968).
35. Kordes, E., Z. Kristall., 91, 65, (1935) as quoted by Bloom and Goldenberg, (Ref. 30).
36. Kubaschewski, O., and Hopkins, B.E., Oxidation of Metals and Alloys, Butterworths, 1967.
37. Cathcart, J.V., in Oxidation of Metals and Alloys, American Society for Metals, 1971, pp. 17-36.

APPENDIX I.

LIST OF ALL TESTS PERFORMED

All fatigue tests were carried out at a cyclic frequency of 1 Hz. using a sinusoidal waveform.

Approximately 10 preliminary tests were run to establish  and achieve familiarization. These tests  unnotched specimens for lives ranging  of 10^6 cycles. All tests reported below were on notched specimens. Tests were terminated when a crack became obviously fatal or, in the majority of cases after 4,000 cycles as noted in the table. The peak stress reported in the table is the nominal peak tensile stress during the load cycle. The minimum stress used was 31,000 psi. compression.

<u>Test No.</u>	<u>Environment</u>	<u>Peak Stress</u>	<u>No. of cycles</u>
1	air	87,500 psi.	15,000
2	air	60,870 psi.	68,000
3	oil	76,090 psi.	4,500
4	dry H ₂	73,000 psi.	24,000
5	wet H ₂	"	19,500
6	air	"	11,500
7	air	"	4,000
8	wet H ₂	"	"
9	dry H ₂	"	"

APPENDIX I. (cont'd)

<u>Test No.</u>	<u>Environment</u>	<u>Peak Stress</u>	<u>No. of cycles</u>
10	dry H ₂	73,000 psi.	4,000
11	dry H ₂	(test invalid)	
12	dry H ₂	73,000 psi..	4,000
13	wet H ₂	(test invalid)	
14	dry H ₂	73,000 psi.	4,000
15	wet H ₂	"	"
16	wet H ₂	"	"
17	wet H ₂	"	"
18	wet H ₂	"	"
19	air	"	"
20	dry H ₂	"	"
21	dry H ₂	"	"
22	dry H ₂	"	"
23	dry H ₂	"	"
24	dry H ₂	"	"
25	dry H ₂	"	"
26	dry H ₂	"	"
27	wet H ₂	"	"
28	wet H ₂	"	"
29	wet H ₂	"	"